Available online at www.sciencedirect.com
SCIENCE DIRECT®
International Journal of Solids and Structures 43 (2006) 3692–3704
INTERNATIONAL JOURNAL OF SOLIDS and STRUCTURES
www.elsevier.com/locate/ijsolstr

Elastic perfectly-plastic asymptotic mixed mode crack tip fields in plane stress

M. Rahman, J.W. Hancock *

Department of Mechanical Engineering, University of Glasgow, University Avenue, Glasgow G128QQ, Scotland, United Kingdom

Received 25 May 2005
Available online 27 July 2005

Abstract

Elastic perfectly-plastic asymptotic plane stress crack tip fields have been constructed by assembling elastic, constant stress and fan sectors under a complete range of mixed mode I/II states of loading. The angular stress distributions are fully continuous, and do not contain the stress discontinuities which have been a feature of many previously proposed solutions. The analytic solutions are verified by finite element solutions under contained yielding conditions. The structure of the elastic perfectly-plastic fields is compared to the structure of the asymptotic strain hardening fields.

Keywords: Crack; Plane stress; Slip line fields

1. Introduction

Insight into the structure of asymptotic elastic–plastic crack tip fields can be developed by idealising the material response as elastic perfectly-plastic. This simplification allows the use of slip field theory, which has been rigorously established for both plane stress and plane strain conditions by Hill (1950). Perfect plasticity has been widely regarded as the limit of a power hardening response as the strain hardening rate approaches zero. In this context, asymptotic perfectly-plastic fields for plane strain and plane stress have been discussed as the limit of the HRR fields (Hutchinson, 1968a; Rice and Rosengren, 1968). However, as the HRR fields are derived for deformation plasticity, or non-linear elasticity, this approach necessarily leads to fields in which plasticity is assumed to surround the crack tip at all angles. As an example, under elastic perfectly-plastic conditions Hutchinson (1968b) has proposed the mode I, plane stress field shown in

* Corresponding author. Tel.: +44 141 330 4722; fax: +44 141 330 4885.
E-mail address: j.hancock@mech.gla.ac.uk (J.W. Hancock).

0020-7683/$ - see front matter
doi:10.1016/j.ijsolstr.2005.05.051

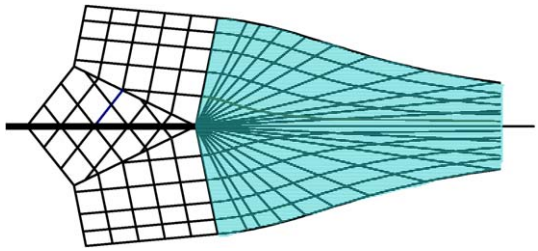

Fig. 1. Hutchinson (1968b) mode I plane stress slip line field. The centred fan sectors are shaded.

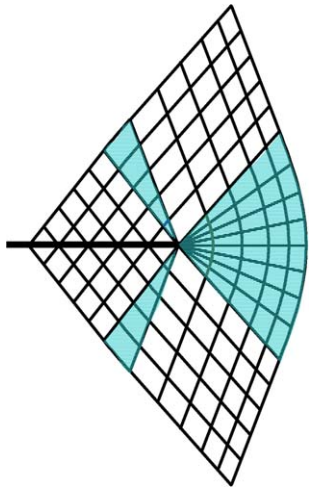

Fig. 2. The Shih (1973) mode II plane stress slip line field. The centred fan sectors are shaded.

Fig. 1. To ensure that the yield criterion is satisfied at all angles around the crack tip it is necessary to introduce a discontinuity in radial stress between the constant stress sectors which trail the crack tip. These discontinuities appear as abrupt changes in the slope of the slip lines. The mode I field was modified by Shih (1973) to accommodate mixed mode I/II loading by postulating that the curved fan ahead of the crack rotates and a constant stress sector develops, splitting the fan ahead of the crack. However discontinuities are still required to satisfy the yield criterion and insufficient equations exist to define their orientation in a unique manner. This problem was addressed by Dong and Pan (1990) who proposed a slightly different arrangement of sectors satisfying the yield criterion at all angles. In mode I this requires a small constant stress sector with an angular span of 5.22° to be introduced directly ahead of the crack. This makes relatively little difference to the mode I stress distribution proposed by Hutchinson (1968b), and in mixed mode loading the sector rotates and expands allowing a unique solution to the orientation of the stress discontinuity. With increasing amounts of shear the discontinuity disappears into the crack flanks giving the fully continuous near mode II fields shown in Fig. 2, discussed by Shih (1973).

The fields proposed by Hutchinson (1968b), Shih (1973) and Dong and Pan (1990) are all based on the assumption that plasticity surrounds the crack tip at all angles. Under perfectly-plastic conditions in plane strain, Nemat-Nasser and Obata (1984), Du and Hancock (1991), Li and Hancock (1999) and Sham et al. (1999) have demonstrated that incomplete plasticity occurs around the crack tip in mode I. Sham and

Hancock (1999) subsequently demonstrated that this is also a feature of the mode I perfectly-plastic plane stress field. In the present work, the assumption that plasticity surrounds the crack tip is relaxed in considering the full family of mixed mode plane stress fields from mode I to mode II, within a framework of small deformation theory. The analytic elastic perfectly-plastic solutions are verified by numerical solutions based on boundary layer formulations. The numerical solutions are extended to strain hardening behaviour and comparisons between the structure of elastic perfectly-plastic and strain hardening fields are discussed as the strain hardening approaches non-hardening behaviour.

2. Slip line fields

Mathematically, slip lines are the characteristics of the governing partial differential equations of equilibrium and compatibility. Under plane stress, the governing equations may be either hyperbolic, parabolic or elliptic, depending on the combination of stresses and the resulting position on the yield surface. Under hyperbolic conditions plane stress slip lines comprise a non-orthogonal grid in which the direct stress across the lines is twice that along the lines. Consequently, the slip lines are lines of zero extension. The angle between the lines depends on the stress state, but in the limit may become zero to give a single set of characteristics when the equilibrium equations are parabolic. For completeness it should be mentioned that in the elliptic case the slip lines are imaginary, as opposed to real. The discussion is developed using cylindrical coordinates (r,θ) centred at the crack tip such that the crack flanks lie along $\theta = \pm\pi$. With this notation, Rice (1982) has shown that under plane stress conditions, the assumption that the crack tip stresses are finite, plus the incompressibility condition and the yield criterion, allows the asymptotic equilibrium equations to be reduced to

$$\frac{\partial \sigma_{\mathrm{m}}}{\partial \theta} \cdot \frac{\partial s_{rr}}{\partial \theta} = 0 \tag{1}$$

where σ_{m} is the mean stress and s_{rr} is the radial stress deviator. The equation has two simple solutions subject to the condition that the yield criterion is satisfied. The condition that the mean stress is independent of angle gives rise to constant stress sectors, in which the slip lines are straight, but non-orthogonal. The condition that the radial stress deviator does not vary with angle, identifies curved fan sectors which comprise straight radial lines intersected by a set of curved characteristics with an equation of the form

$$r^2 \sin(\theta - \phi) = \text{constant} \tag{2}$$

where ϕ is the angle to which the curved lines are asymptotic. A fully developed curved fan is shown in Fig. 3. At the asymptotic angle the two sets of slip lines merge and the equilibrium equations become parabolic. The stresses may be expressed as

$$\sigma_{rr} = \pm k \cos(\theta - \phi) \tag{3.1}$$

$$\sigma_{\theta\theta} = \pm 2k \cos(\theta - \phi) \tag{3.2}$$

$$\sigma_{r\theta} = \pm k \sin(\theta - \phi) \tag{3.3}$$

The alternative solution to Eq. (1) is a sector in which the mean stress is independent of angle and the Cartesian stresses σ_{11}, σ_{22} and σ_{12} are constant, subject to the requirement that the yield criterion is satisfied. The angle between the characteristics can be determined by using the stress–strain relations in conjunction with the stress transformation equations. An important case arises in uniaxial tension or compression, where the slip lines are symmetrically disposed at $\pm 54.7°$ and $\pm 125.3°$ to the direction of uniaxial stress.

Finally the stresses within an elastic sector can be expressed in terms of the semi-infinite wedge solution given by Timoshenko and Goodier (1970), subject to the requirement that the yield criterion is not violated

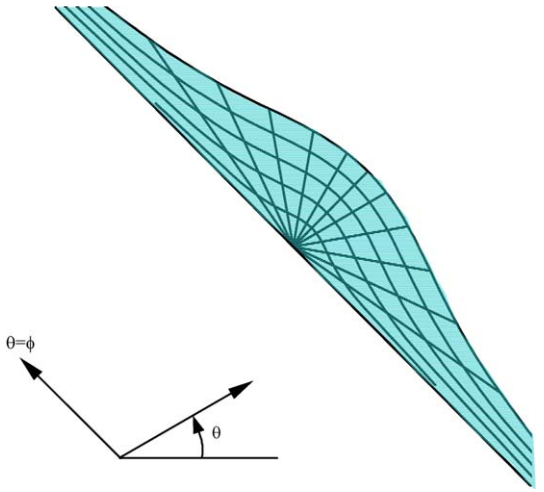

Fig. 3. A fully developed curved fan.

$$\sigma_{rr} = A_1 \sin 2\theta + A_2 \cos 2\theta + (A_3\theta + A_4)/2 \tag{4.1}$$

$$\sigma_{\theta\theta} = -A_1 \sin 2\theta - A_2 \cos 2\theta + (A_3\theta + A_4)/2 \tag{4.2}$$

$$\sigma_{r\theta} = A_1 \cos 2\theta - A_2 \sin 2\theta - A_3/4 \tag{4.3}$$

where A_1, A_2, A_3, and A_4 are constants which are to be determined by the boundary conditions on the sector. In the present work elastic sectors arise on the crack flanks ($\theta = \pm\pi$) where traction free conditions give the relations

$$A_3 = 4A_1 \tag{5.1}$$

$$A_4 = 2(A_2 \pm 2\pi A_1) \tag{5.2}$$

3. Assembly of sectors

The sectors can be assembled subject to the boundary conditions and continuity of tractions across the sector boundaries. Continuity of tractions does not in itself require continuity of all the stress components. Traction continuity requires $\sigma_{\theta\theta}$ and $\sigma_{r\theta}$ to be continuous across the sector boundaries, while an argument presented by Sham and Hancock (1999) shows that σ_{rr} must also be continuous across a boundary between an elastic sector and a fan. The boundary conditions require traction free conditions on the crack flanks and the loading is defined by the ratio of tension to shear directly ahead of the crack. This is defined in terms of a plastic mixity M^{p} introduced by Shih (1973, 1974)

$$M^{\mathrm{p}} = \frac{2}{\pi}\tan^{-1}\left(\frac{\sigma_{\theta\theta}}{\sigma_{r\theta}}\right) \tag{6}$$

Solutions are presented for the values of the plastic mixity listed in Table 1 for which the sector angles on the slip line fields are given in Table 2. It is argued that near mode I fields consist of a curved fan complemented by elastic sectors to the crack flanks as illustrated in Figs. 4(a) and 5(a). The method of solution starts by determining the asymptotic angle ϕ in the fan directly ahead of the crack for a defined plastic mix-

Table 1
Elastic and plastic mixities in plane stress

Loading mode	Elastic mixity (M^{el})	Plastic mixity (M^{p})
K_I	1	1
$K_I/K_{II} = 1$	0.50	0.58
$K_I/K_{II} = 0.45$	0.27	0.38
$K_I/K_{II} = 0.25$	0.16	0.23
K_{II}	0	0

Table 2
Sector angles of the slip line fields in plane stress conditions

	Sector angle (anti-clockwise positive) in degrees							
	θ_1	θ_2	θ_3	θ_4	θ_5	θ_6	θ_7	θ_8
K_I	−39.126	39.126						
$K_I/K_{II} = 1$	−69.6	53.34						
$K_I/K_{II} = 0.45$	−180	−125.3	54.7	180				
$K_I/K_{II} = 0.25$	−180	−125.3	−97.83	−51.92	52.77	118.6	125.3	180
K_{II}	−180	−125.3	−109.32	−51.21	51.21	109.32	125.3	180

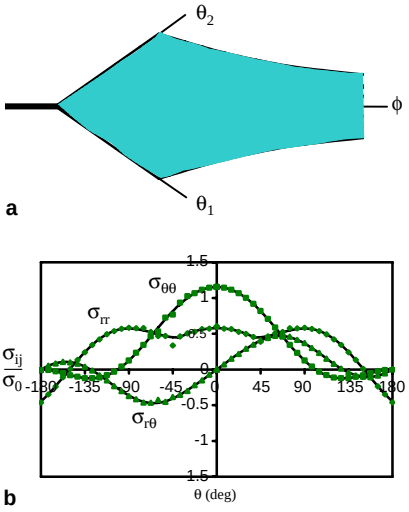

Fig. 4. (a) Sham and Hancock (1999) mode I plane stress slip line field. (b) Sham and Hancock (1999) mode I plane stress field. The data points are numerical results while the solid lines represents the analytic solution.

ity. In the fields presented the plane directly ahead of the crack always lies in a curved fan sector in accord with an assumption of Shih (1973), but in contrast to the fields discussed by Dong and Pan (1990). This allows the relation between the asymptotic fan angle ϕ and the plastic mixity to be written as

$$\phi = \tan^{-1}\left(2\cot\left(\frac{\pi M^{p}}{2}\right)\right) \tag{7}$$

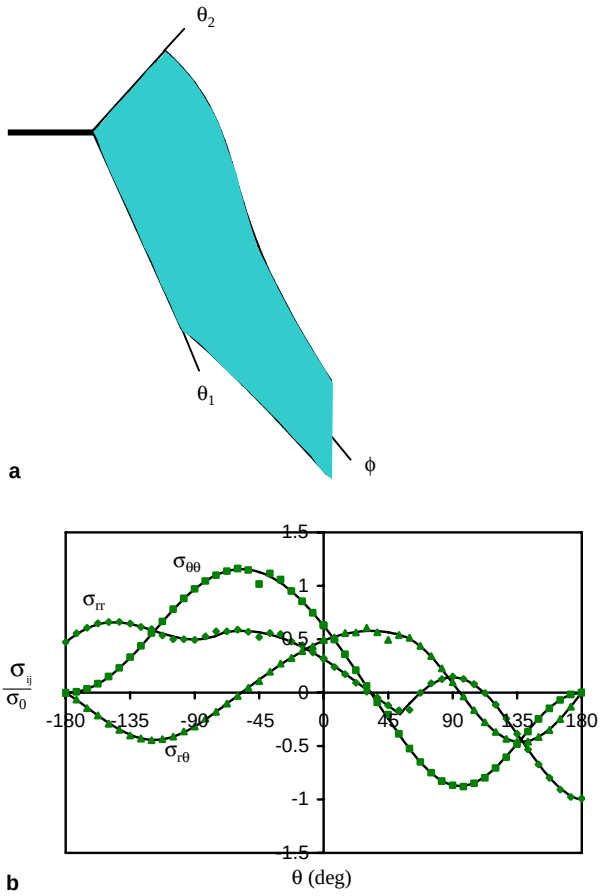

Fig. 5. (a) Slip line field at the crack tip under plane stress mixed mode ($K_I/K_{II} = 1$) loading. (b) Stress field at the crack tip under plane stress mixed mode loading ($K_I/K_{II} = 1$). The data points are numerical results while the solid lines represents the analytic solution.

Continuity of stresses σ_{rr}, $\sigma_{\theta\theta}$ and $\sigma_{r\theta}$ across the sector boundary at θ_2 allows Eqs. (3.1)–(3.3) to be combined with Eqs. (4.1)–(4.3) and (5.1) and (5.2) to give three equations which can be solved simultaneously to define the sector boundary θ_2 and the two unknown constants A_1 and A_2. An identical argument gives the corresponding sector boundary θ_1 between the fan and the elastic sector on the lower flank. Finally it is necessary to check a posteriori that the stresses postulated in any elastic sectors do not violate the yield criterion.

The mode I field, which is shown in Fig. 4(a) and discussed in detail by Sham and Hancock (1999), can be regarded as a limiting case of a near mode-I field. The field consists of a curved fan sector directly ahead of the crack in the angular range $\theta = \pm 39.126°$ complemented by elastic sectors extending to the crack flanks. The mode I stress field is shown in Fig. 4(b). Under mixed mode loading, the near mode I fields consist of a simple modification to this such that the curved fan rotates, but remains complemented by asymmetric elastic sectors to the crack flanks. As an example a mixed mode field corresponding to a remote ratio $K_I/K_{II} = 1$ and plastic mixity, 0.58 is shown in Fig. 5(a). The field consists of a curved fan which extends between 53.34° and −69.6°. The slip lines in the fan are asymptotic to −57.17° while elastic sectors extend to the crack flanks. The corresponding stress field is shown in Fig. 5(b).

A critical transitional field arises when the angle of the elastic wedge on the upper crack flank reaches 54.7° and the asymptotic fan angle $\phi = -70.53°$ and the plastic mixity M^p is 0.392. The yield criterion is

violated in any postulated elastic sector between the fan and the crack flanks, but the field can be completed by a constant stress sector extending from 54.7° to the upper flank. The stress within this sector is a simple uniaxial compression parallel to the crack flanks

$$\sigma_{rr} = -\sqrt{3}k\cos^2\theta \tag{8.1}$$

$$\sigma_{\theta\theta} = -\sqrt{3}k\sin^2\theta \tag{8.2}$$

$$\sigma_{r\theta} = \frac{\sqrt{3}}{2}k\sin 2\theta \tag{8.3}$$

where $54.7° \leqslant \theta \leqslant 180°$.

On the lower flank a constant stress sector emerges in the angular range $-125.3° \geqslant \theta \geqslant -180°$ from the fan to the crack flank. The remote loading condition, $K_I/K_{II} = 0.45$, gives a plastic mixity M^p is 0.38 which is very close to the critical configuration, at which plasticity breaks through to the upper and lower crack flanks. This slip line field is illustrated in Fig. 6(a) and the corresponding stress field is given in Fig. 6(b).

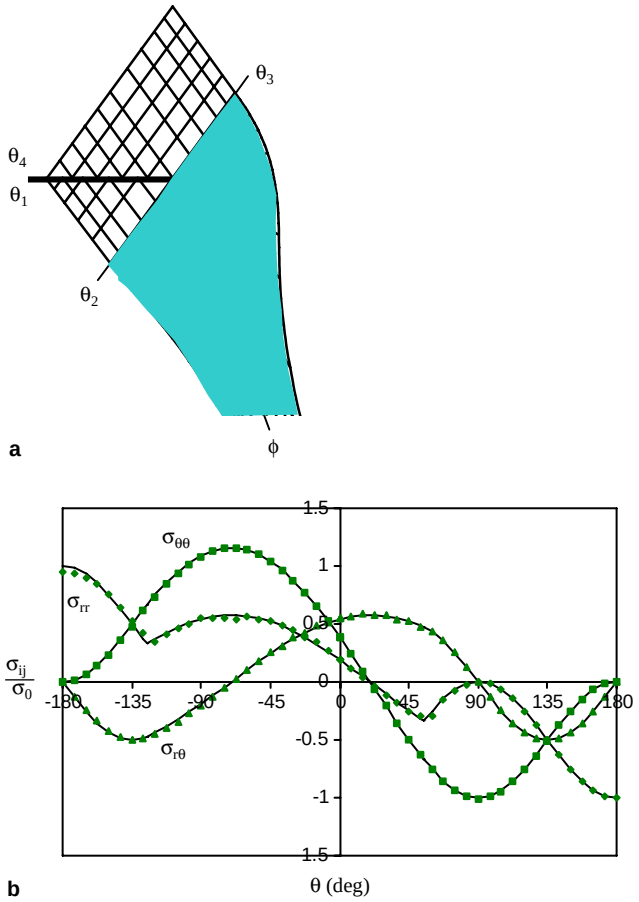

Fig. 6. (a) Slip line field at the crack tip under plane stress mixed mode ($K_I/K_{II} = 0.45$) loading. The centred fans are shaded for clarity. (b) Stress field at the crack tip under plane stress mixed mode ($K_I/K_{II} = 0.45$) loading. The data points are numerical results while the solid lines represent the analytic solution.

With increased levels of applied shear a fan emerges at 125.3° and a constant stress sector develops at −70.53° which is the asymptotic angle of the fan ahead of the crack. This gives rise to the near mode II fields. Near mode II fields consist of constant stress sectors on the upper and lower flanks leading to curved fan sectors and two further constant stress sectors which adjoin a curved fan directly ahead of the crack as shown in Fig. 7(a). The method of solution starts by determining the asymptotic fan angle ($\phi = \phi_1$) for the fan directly ahead of the crack using Eqs. (6) and (7). The constant stress sector angle $\theta_7 = 125.3°$ and continuity of stress across this sector boundary gives the asymptotic fan angle ($\phi = \phi_2$) for the fan, which initially emerges at 125.3°, as 70.53°. The field above the crack plane is fixed by the span of the constant stress sector between θ_5 and θ_6. The angle between the slip lines in a constant stress sector gives the relation

$$\tan(\theta_6 - \theta_5) = 2\tan(\phi_1 - \phi_2) \tag{9}$$

while equating the mean stress at θ_5 and θ_6 gives the relation

$$(\theta_5 + \theta_6) = (\pi + \phi_1 + \phi_2) \tag{10}$$

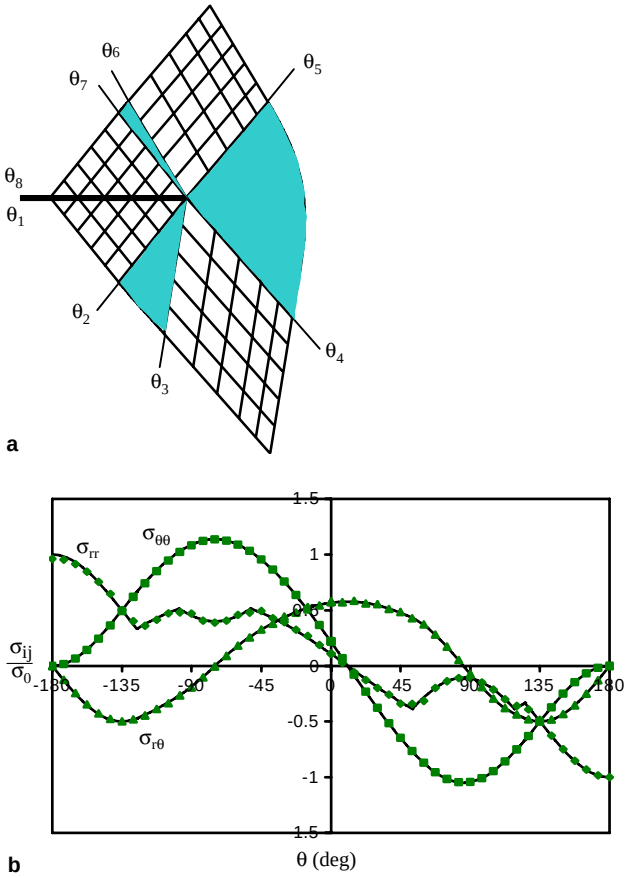

Fig. 7. (a) Slip line field at the crack tip under plane stress mixed mode ($K_I/K_{II} = 0.25$) loading. The centred fans are shaded for clarity. (b) Stress field at the crack tip under plane stress mixed mode ($K_I/K_{II} = 0.25$) loading. The data points are numerical results while the solid lines represent the analytic solution.

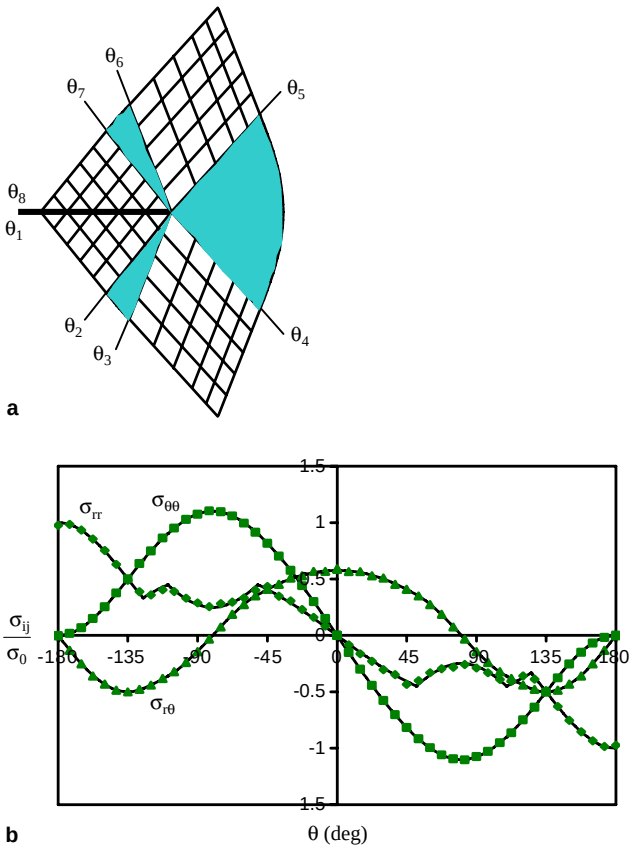

Fig. 8. (a) Slip line field at the crack tip under plane stress mode II loading. The centred fans are shaded for clarity. (b) Stress field at the crack tip under plane stress mode II loading. The data points are numerical results while the solid lines represent the analytic solution.

These equations are solved simultaneously to give numerical values of θ_5 and θ_6. A similar procedure gives the sector boundaries on the lower flank. For the remote loading condition, $K_I/K_{II} = 0.25$, $M^p = 0.23$, the slip line field is shown in Fig. 7(a) and the corresponding stress field in Fig. 7(b). Finally in pure shear, $K_I/K_{II} = 0$, the anti-symmetric field, identified by Shih (1973) emerges, for which the slip line field is shown in Fig. 8(a) and corresponding stress field is given in Fig. 8(b).

4. Boundary layer formulations

To verify the analytical solutions, a finite element technique based on modified boundary layer formulations (Rice and Tracey, 1973) has been used to obtain numerical solutions for contained yielding. Cartesian displacements corresponding to the stress intensity factors for a general mixed mode loading were obtained by superimposing the displacements $u_1^{K_I}$ and $u_2^{K_I}$, for a mode I field with those associated with a mode II field $u_1^{K_{II}}$ and $u_2^{K_{II}}$

$$u_1 = u_1^{K_I} + u_1^{K_{II}} \tag{11.1}$$

$$u_2 = u_2^{K_I} + u_2^{K_{II}} \tag{11.2}$$

where

$$u_1^{K_I} = \frac{K_I}{2G}\left(\frac{r}{2\pi}\right)^{\frac{1}{2}}\left(\cos\frac{\theta}{2}\left(\kappa - 1 + 2\sin^2\frac{\theta}{2}\right)\right) \tag{12.1}$$

$$u_2^{K_I} = \frac{K_I}{2G}\left(\frac{r}{2\pi}\right)^{\frac{1}{2}}\left(\sin\frac{\theta}{2}\left(\kappa + 1 - 2\cos^2\frac{\theta}{2}\right)\right) \tag{12.2}$$

$$u_1^{K_{II}} = \frac{K_{II}}{2G}\left(\frac{r}{2\pi}\right)^{\frac{1}{2}}\left(\sin\frac{\theta}{2}\left(\kappa + 1 + 2\cos^2\frac{\theta}{2}\right)\right) \tag{12.3}$$

$$u_2^{K_{II}} = \frac{K_{II}}{2G}\left(\frac{r}{2\pi}\right)^{\frac{1}{2}}\left(-\cos\frac{\theta}{2}\left(\kappa - 1 - 2\sin^2\frac{\theta}{2}\right)\right) \tag{12.4}$$

K_I and K_{II} are the mode I and mode II stress intensity factors, r is the distance from the crack tip, $\kappa = (3 - \nu)/(1 + \nu)$, ν is Poisson's ratio and G is the shear modulus. Numerical solutions were developed with a Poisson's ratio of 0.49, giving a response which is close to incompressible. In order to verify the analytic solutions, finite element solutions have been determined for specific ratios of elastic mixity defined by the ratio (K_I/K_{II}) or by an elastic mixity, M^{el} as given in Table 1.

$$M^{el} = \frac{2}{\pi}\tan^{-1}\left(\frac{K_I}{K_{II}}\right) \tag{13}$$

The calculations have generally been performed using boundary layer formulations in which the displacements associated with the leading singularity are applied to the outer boundary of the mesh. However, the second order term in the asymptotic expansion of the elastic field (Williams, 1957), known as the T-stress is known to have strong effect on plane strain fields (Du and Hancock, 1991). As a result a limited number of calculations were performed using displacements corresponding to the first two terms of the expansion of the asymptotic elastic field given by Williams (1957). The displacements associated with the T-stress are

$$u_1^T = \frac{Tr\cos\theta}{E} \tag{14.1}$$

$$u_2^T = -\frac{\nu Tr\sin\theta}{E} \tag{14.2}$$

where E is Young's Modulus.

The crack-tip fields have been modelled by using a highly focused mesh based on 24 rings of 24 isoparametric second-order hybrid elements concentric with the crack tip. The crack tip thus consists of 49 initially coincident, but independent nodes. Under elastic perfectly-plastic conditions the asymptotic crack tip stresses are finite, and have been determined numerically by extrapolating the stresses to the crack tip along radial lines at 7.5° intervals around the crack tip. The slip line fields can be constructed from these numerical results using Eq. (1) to identify the constant stress and fan sectors, subject to the condition that the yield criterion is satisfied, while the elastic sectors are identified by the condition that the Mises stress is less than the uniaxial yield stress, σ_0. Figs. 4(b)–8(b), compare the analytic solutions with the numerical results. The numerical results indicated by points and the analytic solutions shown as continuous lines are clearly in excellent agreement. The T-stress modifies the relation between the elastic and plastic mixities, but has little effect on the asymptotic mode I stress field. However, it does affect the size and shape of the plastic zone at the crack tip as shown in Fig. 9. Negative (compressive) T-stresses enlarge the plastic zone which forms two distinct lobes ahead of the crack tip, while tensile T-stresses enlarge the plastic zone on the crack plane.

Strain hardening solutions have been obtained for a strain hardening response which in uniaxial tension is linearly elastic below the yield stress σ_0, and merges into a Ramberg–Osgood power hardening relationship above the yield stress. Numerical calculations have been performed for strain hardening exponents

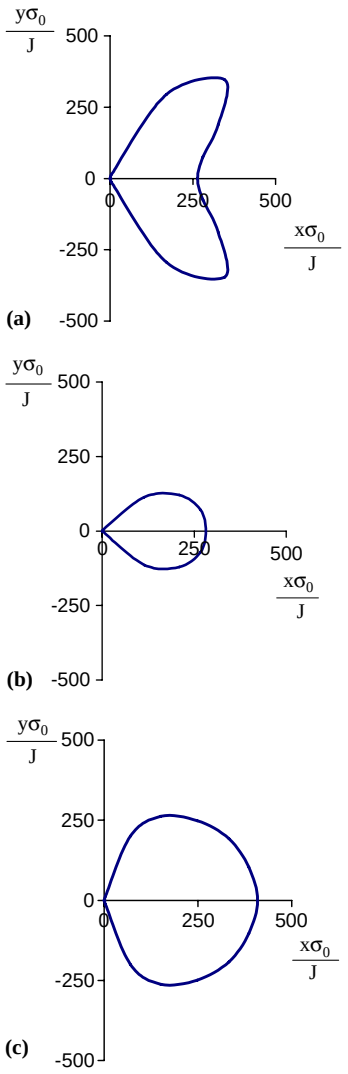

Fig. 9. Effect of the T-stress on the plastic zone at the crack tip under plane stress mode I loading. (a) $T = -0.5\sigma_0$, (b) $T = 0$ and (c) $T = +0.5\sigma_0$.

$n = 0.05$ and 0.1 which represent a weak and a moderate strain hardening responses. For a strain hardening response the HRR fields define the strength of the dominant singularity. However as all the stress components have the same radial dependence, the stresses normalised by the corresponding local Mises stress are finite. Non-dimensionalised in this way the stresses can be extrapolated to the crack tip in the same way that the stresses normalised by the yield stress were extrapolated to the tip for an elastic perfectly-plastic response. In order to show the structure of the strain hardening fields interest is focussed on the asymptotic mean stress, σ_{m} and the radial stress deviator, s_{rr} normalised by the Mises stress. These are plotted for two strain-hardening rates in Figs. 10(a) and (b). The numerical solutions are compared with the mode I elastic perfectly-plastic solution proposed by Hutchinson (1968b) which is indicated by a solid line, while the numerical data are indicated by points.

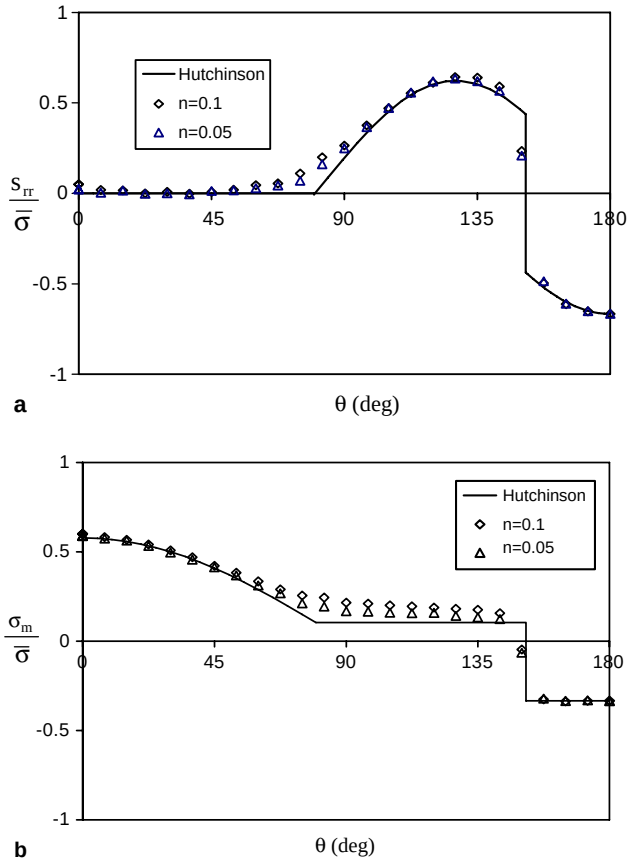

Fig. 10. (a) Comparison of radial stress deviators in the Hutchinson (1968b) mode I field and in mode I hardening solutions in plane stress. The discontinuity in the Hutchinson field occurs at 151.4°. (b) Comparison of mean stresses in Hutchinson (1968b) mode I field and in mode I hardening solutions in plane stress. The discontinuity in the Hutchinson field occurs at 151.4°.

5. Discussion

Elastic perfectly-plastic fields are often regarded as the non-hardening limit of the HRR fields. However the absence of strain hardening permits the existence of elastic sectors in which the yield criterion is not satisfied. In near mode I this leads to fields comprising a curve fan complemented by elastic sectors on the crack flanks. The fan rotates with increasing mode II loading until a critical configuration arises when constant stress sectors break through to the crack flanks. With increased levels of shear, additional constant stress and curved fan sectors emerge, leading to the near mode II fields discussed by Shih (1973). All the fields in the family of fields exhibit full continuity of stresses.

The structure of the plane stress strain hardening fields can be related to those for perfectly-plastic conditions by examining the angular variation of mean stress and the radial stress deviator normalised by the Mises stress as shown in Fig. 10(a) and (b). In perfectly-plastic conditions the fields consist of assemblies of curved fan, constant stress, and elastic sectors. In numerical solutions the fans can be identified as sectors in which the radial stress deviator s_{rr} is zero. This feature is retained in strain hardening and a fan-like feature extends directly ahead of the crack tip with a similar span to that found in perfect plasticity. Unlike the perfectly-plastic solution strain hardening causes plasticity to encompass the crack tip at all angles. In

perfect-plasticity constant stress sectors exhibit a mean stress which is invariant with angle. This feature is also shown by the strain hardening solutions in Fig. 10(b) which show two constant stress like features. One extends from crack flanks to an angle close to 150° and another sector extends from 150° to adjoin the fan-like feature. The constant stress sectors are separated by a narrow zone featuring very high angular stress gradients. The perfectly-plastic solution of Hutchinson (1968b) has been plotted in both Figs. 10(a) and (b), in which plasticity is assumed to surround the crack tip at all angles. It is clear that the strain hardening solutions tend towards this field as the strain hardening exponent decreases. The stress discontinuity in the Hutchinson solution appears as the zone of high angular stress gradients in the strain hardening solution. However in the limit of perfect-plasticity the nature of the fields abruptly changes as elastic sectors appear on the crack flanks.

Acknowledgements

Moshiur Rahman acknowledges the support of the Bangladesh Atomic Energy Commission. ABAQUS was provided by HKS under academic license from HKS Inc.

References

Dong, P., Pan, J., 1990. Asymptotic crack-tip fields for perfectly plastic solids under plane-stress and mixed-mode loading conditions. Journal of Applied Mechanics 57, 635–638.

Du, Z.-Z., Hancock, J.W., 1991. The effect of non-singular stresses on crack tip constraint. Journal of the Mechanics and Physics of Solids 39, 555–567.

Hill, R., 1950. The Mathematical Theory of Plasticity. Oxford University Press, Oxford.

Hutchinson, J.W., 1968a. Singular behaviour at the end of a tensile crack in a hardening material. Journal of the Mechanics and Physics of Solids 16, 13–31.

Hutchinson, J.W., 1968b. Plastic stress and strain fields at a crack tip. Journal of the Mechanics and Physics of Solids 16, 337–347.

Li, J., Hancock, J.W., 1999. Mode I and mixed mode fields with incomplete crack tip plasticity. International Journal of Solids and Structures 36, 711–725.

Nemat-Nasser, S., Obata, M., 1984. On the stress field near a stationary crack tip. Mechanics of Materials 3, 235–243.

Rice, J.R., 1982. Elastic–plastic crack growth. In: Hopkins, H.G., Sewell, M.J. (Eds.), Mechanics of Solids. The Rodney Hill Anniversary Volume, pp. 539–562.

Rice, J.R., Rosengren, G.F., 1968. Plane strain deformation near a crack tip in a power law hardening material. Journal of the Mechanics and Physics of Solids 16, 1–12.

Rice, J.R., Tracey, D.M., 1973. Numerical and Computational Methods in Structural Mechanics. Academic Press, New York.

Sham, T.L., Hancock, J.W., 1999. Mode I crack tip fields with incomplete crack tip plasticity in plane stress. Journal of the Mechanics and Physics of Solids 47, 2011–2027.

Sham, T.L., Li, J., Hancock, J.W., 1999. A family of plane strain crack tip stress fields for interface cracks in strength-mismatched elastic-perfectly plastic solids. Journal of the Mechanics and Physics of Solids 47, 1963–2010.

Shih, C.F., 1973. Elastic–plastic analysis of combined mode crack problems, Ph.D. Thesis, Harvard University, Cambridge, MA.

Shih, C.F., 1974. Small scale yielding analysis of mixed mode plane-strain crack problems. Fracture Analysis ASTM STP 560, 187–210.

Timoshenko, S.P., Goodier, J.N., 1970. Theory of Elasticity, third ed. McGraw-Hill, New York.

Williams, M.L., 1957. On the stress distribution at the base of a stationary crack. Journal of Applied Mechanics 24, 111–114.